Supplementary Information

Nickel-doped copper oxide nanoparticle synthesized by co-precipitation method for efficient electrocatalytic synthesis of ammonia from nitrate

1. Experimental Procedures

Determination of NH_3

The concentration of ammonia was obtained by using the indophenol blue method in combination with the colorimetric method. To measure the content of NH_3 in the electrolyte after the NO_3^- reduction reaction, Take 1 ml of the electrolyte from the cathode chamber and add it to a 10 ml centrifuge tube, add deionized water to make the volume reach 10 ml, dilute it 10 times, then take 1 ml of the diluted 10-fold solution. Next, add a certain amount of 0.05 M H_2SO_4 solution to the centrifuge tube to make the solution pH close to neutral, and then make the volume reach 10 ml. Obtain the diluted electrolyte solution 100 times its original volume, and then take 1 ml of the diluted electrolyte solution 100 times its original volume and place it in a centrifuge tube, Then, 1 ml of salicylic acid (composed of 40 ml of deionized water, 2 grams of salicylic acid, 2 grams of sodium citrate, and 1.6 grams of NaOH), 0.1 ml of sodium nitroprusside (composed of 10 ml of deionized water and 0.1 gram of sodium nitroprusside), and 0.1 ml of sodium hypochlorite (composed of 10 ml of deionized water, 5 ml of 6-14% sodium hypochlorite, and 0.8 grams of NaOH)were added successively. The solution was then made up to 10 ml and left in the dark for 1 hour for color development.

Subsequently, the absorbance at 665 nm was measured using an ultraviolet-visible spectrophotometer (UV-1800PC). The concentration of ammonia was determined by using the standard curve obtained by combining the absorbance measurements with a series of gradient concentrations of NH_4Cl solutions (Fig. S1a-b).

Determination of NO_2^-

Obtain the concentration information of nitrite by using the Griess chromogenic reagent in conjunction with the colorimetric method. In order to obtain the concentration of nitrite ions in the electrolyte, 1 mL of the electrolyte in the cathode chamber was diluted 100 times. 1 mL of the 100-fold diluted electrolyte was taken and placed in a centrifuge tube. Then, 0.2 mL of Griess reagent (Composed of 50 mL deionized water, 4 g sulfonamide, 0.2 g N-(1-naphthyl) ethylenediamine dihydrochloride, and 10 mL phosphoric acid) was added, and the volume was adjusted to 10 mL. The solution was then exposed to light for 20 minutes for color development (Fig. S1c-d).

The Faradaic efficiency of NO_3RR and NH_3 yield

The Faraday efficiency of ammonia is calculated according to the following formula:

$$FE_{NH_3}=(8 *F *CNH_3*V)/(14 * Q)$$

Here, 8 represents that 1 moL of NO_3^- reacting to form 1 moL NH_3 transfers 8 electrons. F is the Faraday constant (96500 C/mol), cNH_3 represents the concentration of NH_4^+, V represents the volume of the electrolyte at the cathode, 14 represents the relative atomic mass of N, and Q represents the charge consumed during the electrolysis process.

The Faraday efficiency of NO_3^- to NO_2^- can be calculated by the following formula：

$$FE=(2\ F*C_{NO2^-}*V)/(14*Q)$$

Here, 2 indicates that during the reaction of 1 moL NO_3^-, 1 moL of NO_2^- is produced and 2 electrons are transferred. F represents Faraday's constant (96500 C/mol), cNO_2^- represents the concentration of NO_2^-, V represents the volume of the anode electrolyte, 14 represents the mass of N, and Q represents the charge consumed during the electrolysis process.

2. Figures

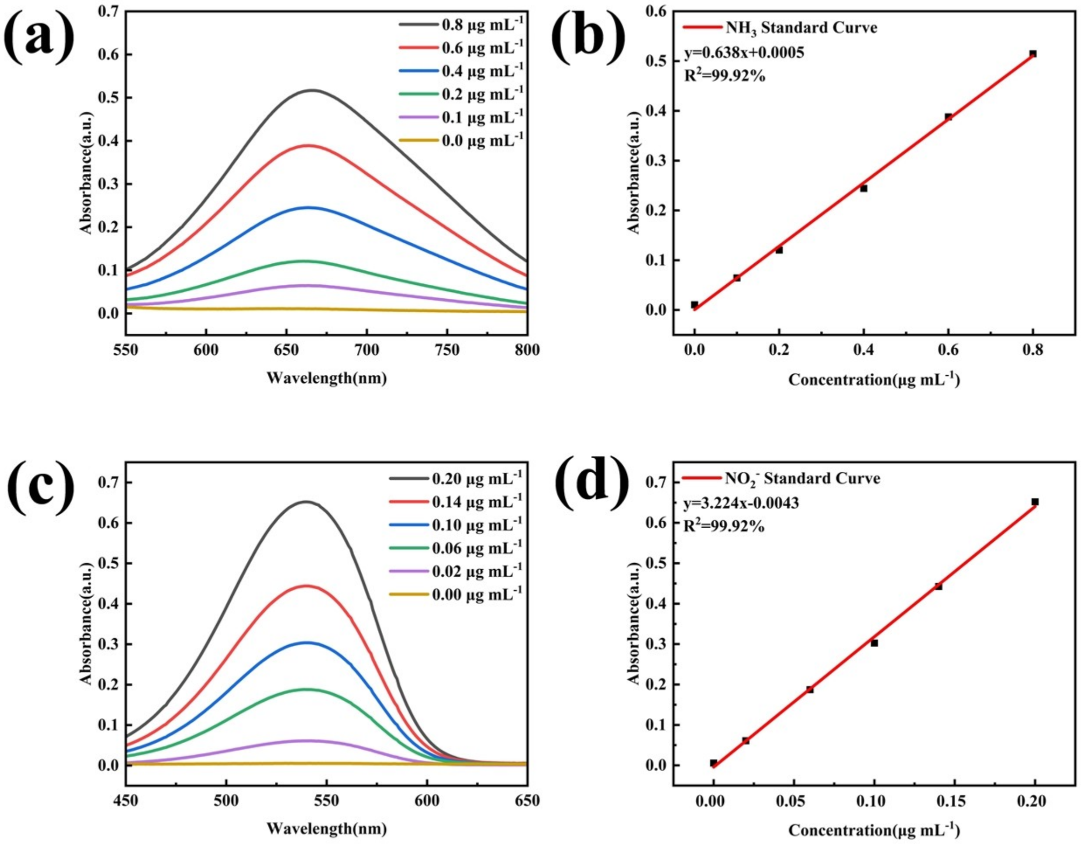

Fig. S1 (a) UV-vis absorption curves of NH_4Cl standard solutions. (b) Linear fitting results of the calibration curve. (c) UV-vis absorption curves of $NaNO_2$ standard solutions. (d) Linear fitting results of the calibration curve.

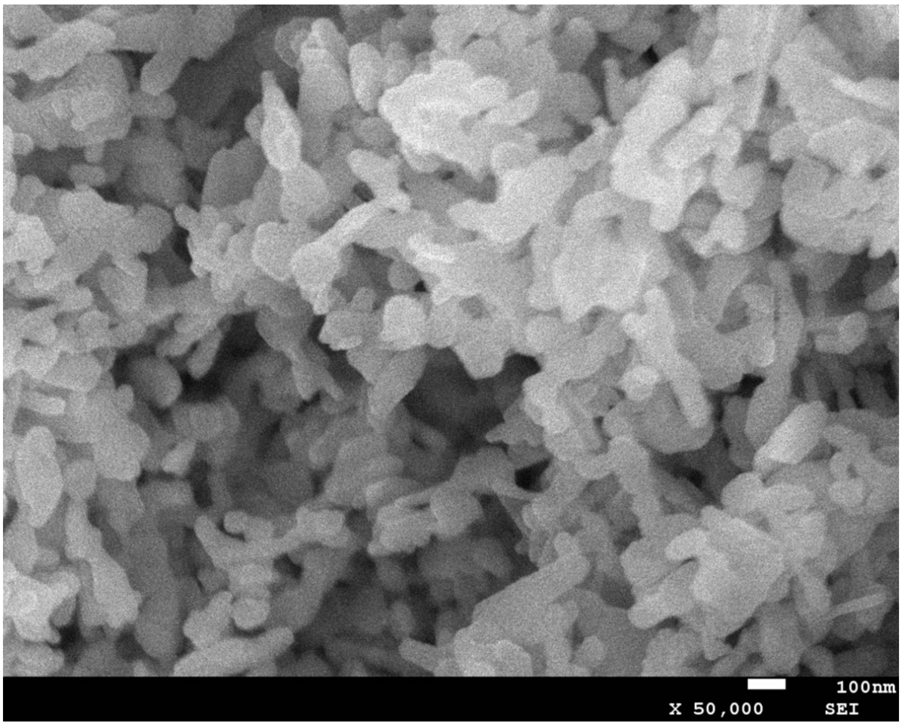

Fig. S2 SEM images of 0.1-Ni-CuO NP.

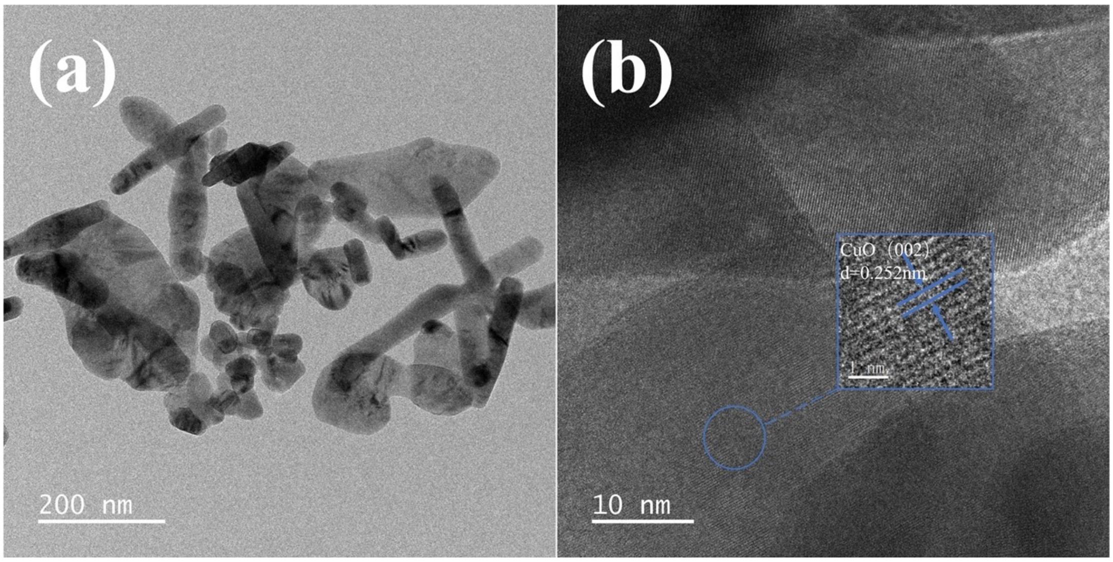

Fig. S3 (a) TEM images of CuO NP. (b) HRTEM images of CuO NP.

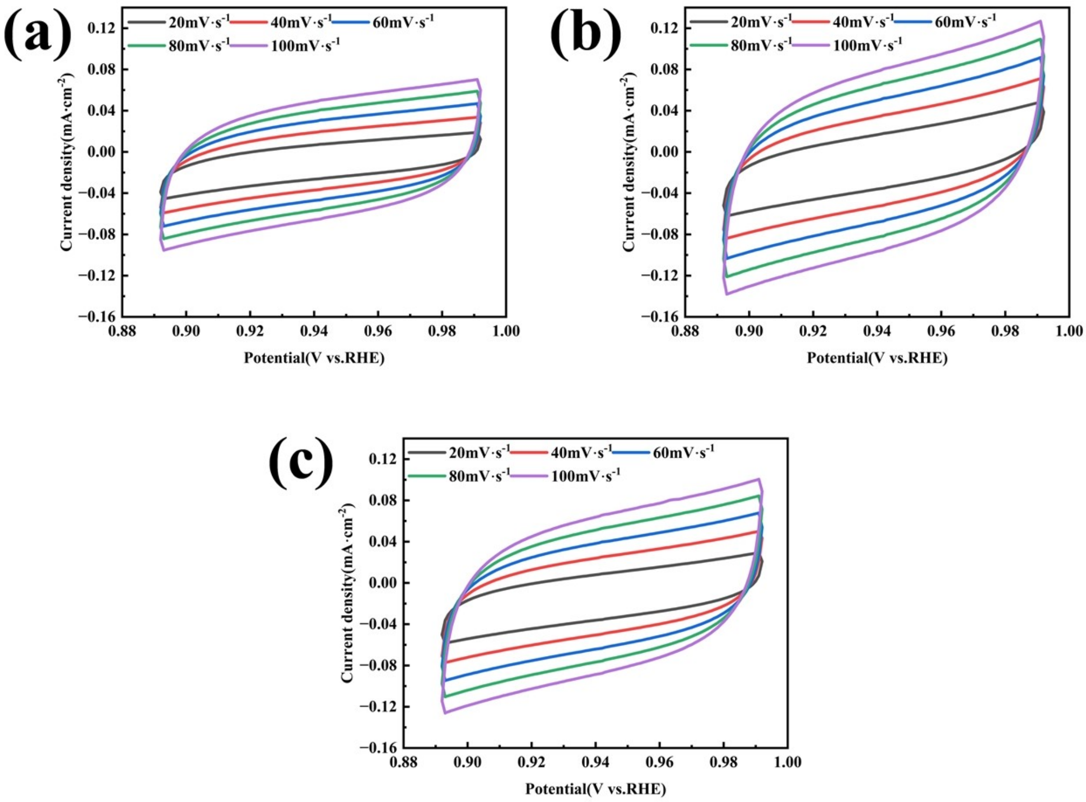

Fig. S4 Cyclic voltammograms (CV) of (a) 0.1-Ni-CuO NP,(b) CuO NP,(c) NiO NP at different scan rates from 20 to 100mV s^{-1} .

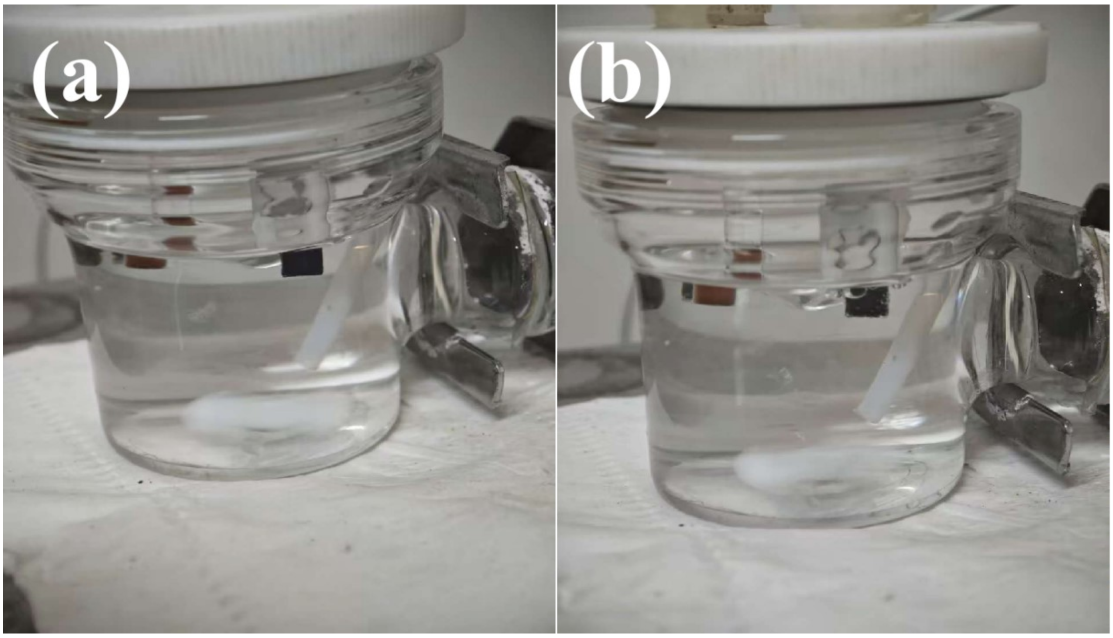

Fig. S5 The production of H_2 on (a) 0.1-Ni-CuO NP and (b) NiO NP.

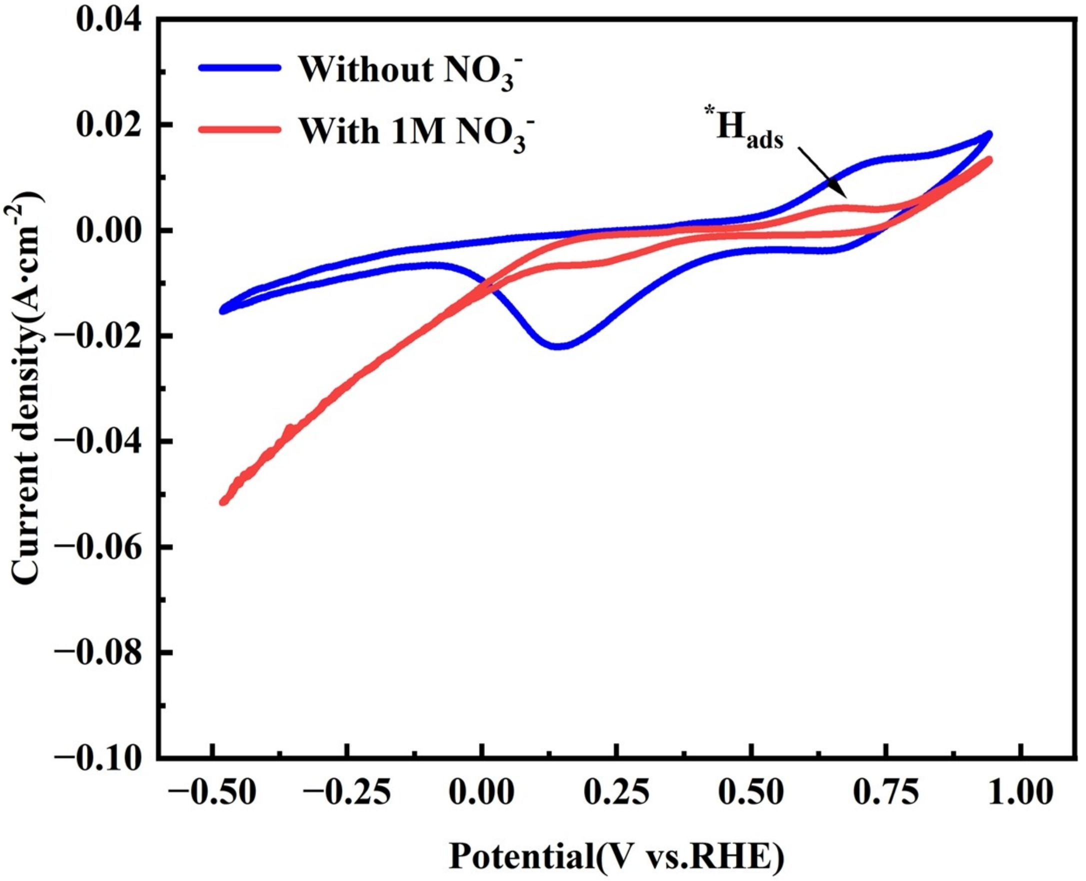

Fig. S6 CV tests of CuO NP at the working potential.

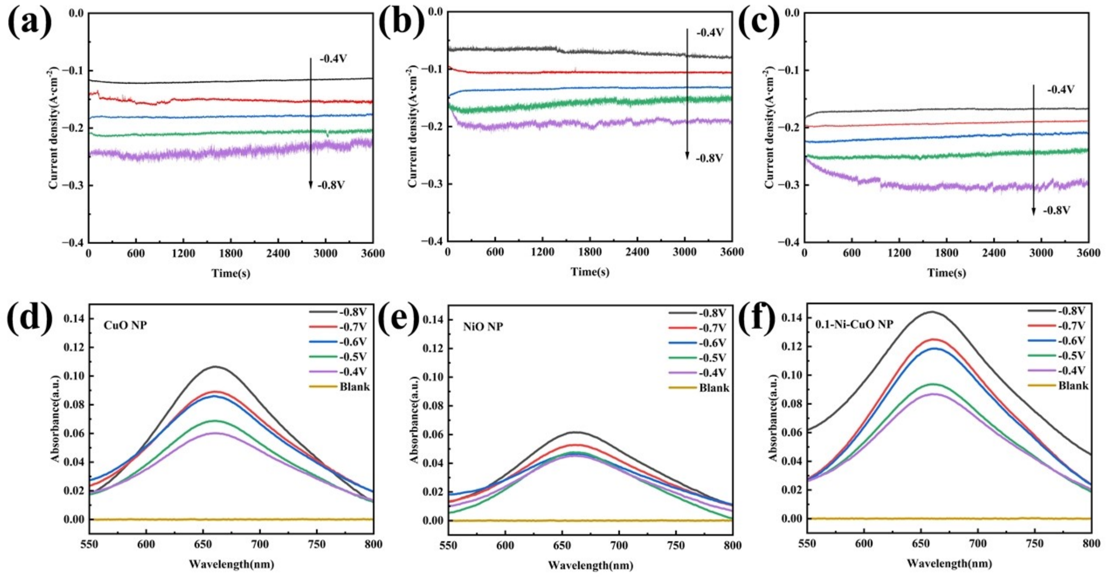

Fig. S7 (a)-(c) i-t curves of CuO NP, NiO NP, 0.1-Ni-CuO NP at different potentials,

(d)-(f) UV–vis absorption curves of electrolytes at different voltages.

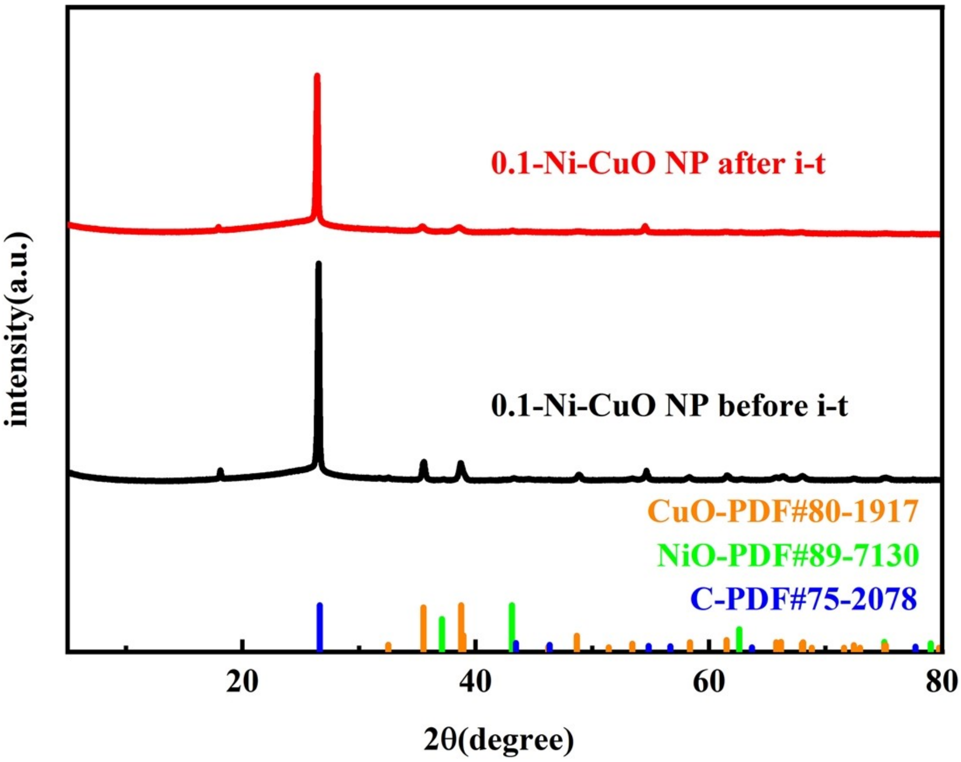

Fig. S8 XRD spectra of 0.1-Ni-CuO NP before and after NO_3RR.

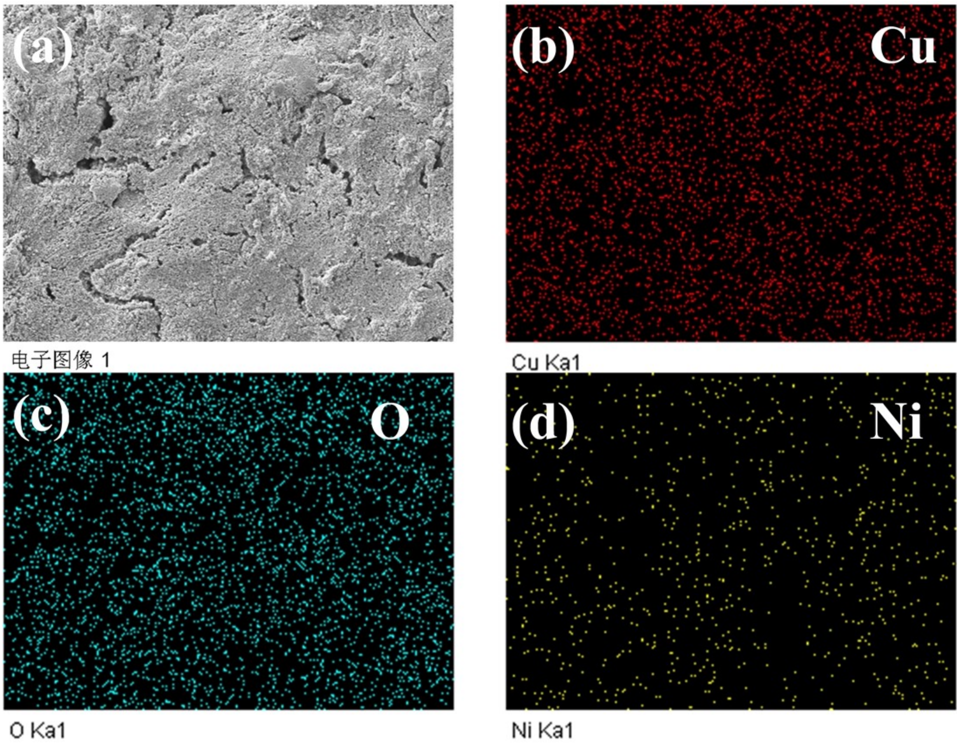

Fig. S9 (a) SEM image of 0.1-Ni-CuO NP after NO_3RR, (b)-(d) EDS image of 0.1-Ni-CuO NP after NO_3RR.

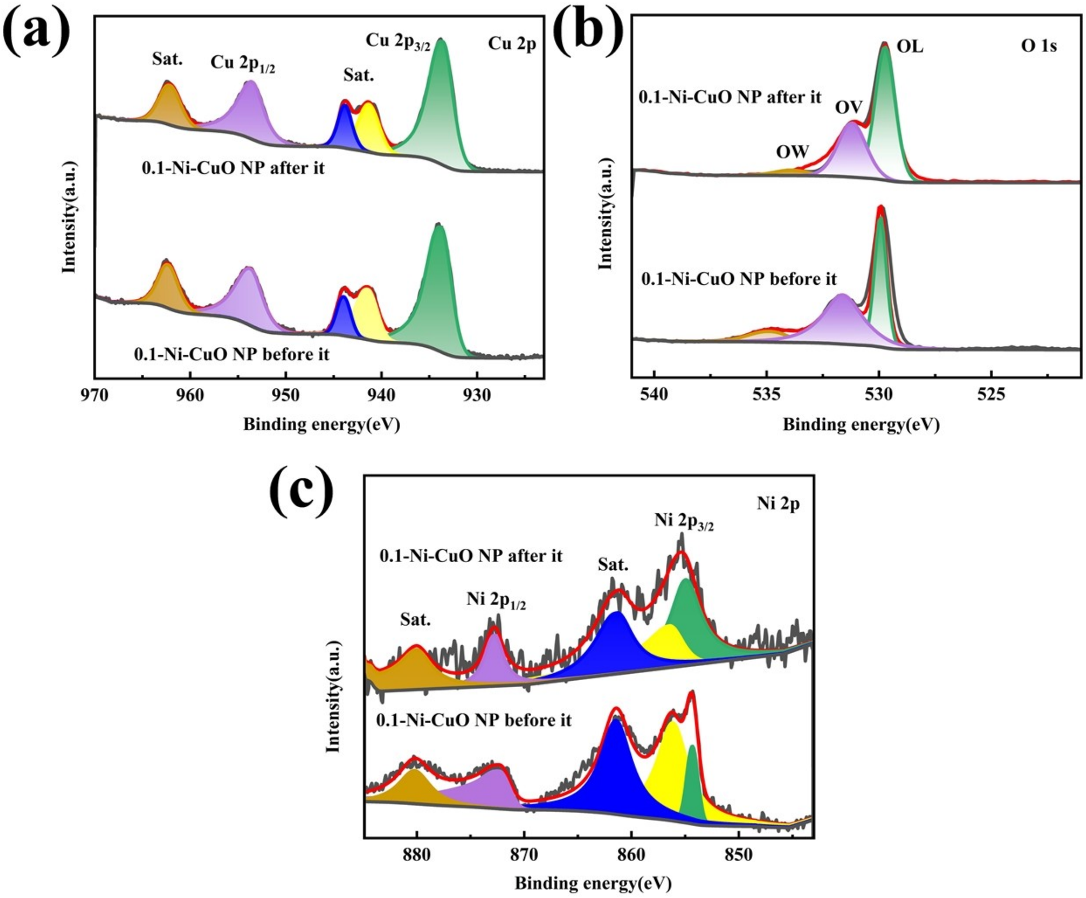

Fig. S10 High-resolution XPS spectra of (a) Cu 2p (b) O 1s (c) Ni 2p for 0.1-Ni-CuO NP before and after NO_3RR.

Tab. S1 The comparison of the NH_3 yields and FEs of 0.1-Ni-CuO NP with the reported catalysts for NO_3RR.

Catalyst	**Electrolyte**	**FE(NH_3）（%）**	**NH_3 Yield**	**Ref.**
Cu nanoparticle	10 mM KNO_3, 0.1 M KOH	61%	225.8 μg $h^{-1}cm^{-2}$	1
Cu SAC	0.1 M KNO_3, 0.1 M KOH	84.70%	0.26 mmol h^{-1} cm^{-2}	2
dr-Cu-NPs	0.5 M K_2SO_4, 50 ppm KNO_3	81.99%	781.25 μg h^{-1} mg^{-1}	3
Cu-incorporated PTCDA	0.1 mMPBS, 36 mMNO_3^-	77%	0.0256 mmol h^{-1} cm^{-2}	4
Cu3Pd1	0.5 M K_2SO_4, 50 ppm KNO_3-N	90.02%	784.37 mg cm^{-2} mg^{-1}	5
$Ag_{20}Cu_{12}$	0.5 M Na_2SO_4, 500 ppm $NaNO_3$	84.60%	0.138 mmol h^{-1} mg^{-1}	6
Cu/CuAu ordered SAA	1 M KOH, 1 M KNO_3	85.50%	8.47 mol g^{-1} h^{-1}	7
np-CuCo	1 M KOH, 200 ppm NO_3	85.20%	275.9 μmol h^{-1} cm^{-2}	8
Cu2O@Pd	0.1 M NaOH, 0.01 M $NaNO_3$	81.20%	1.08 mg $h^{-1}cm^{-2}$	9
CuNi/OMC	0.1 M PBS, 500 ppm KNO_3	78.90%	2.37 mg cm^{-2} h^{-1}	10
0.1-Ni-CuO NP	0.1 M $NaNO_3$, 1 M NaOH	90.60%	1.065 mmol·h^{-1}·cm^{-2}	This work

References

1 X. Fu, X. Zhao, X. Hu, K. He, Y. Yu, T. Li, Q. Tu, X. Qian, Q. Yue, M. R. Wasielewski and Y. Kang, *Applied Materials Today*, 2020, **19**, 100620.

2 J. Yang, H. Qi, A. Li, X. Liu, X. Yang, S. Zhang, Q. Zhao, Q. Jiang, Y. Su, L. Zhang, J.-F. Li, Z.-Q. Tian, W. Liu, A. Wang and T. Zhang, *J. Am. Chem. Soc.*, 2022, **144**, 12062–12071.

3 Y. Xu, M. Wang, K. Ren, T. Ren, M. Liu, Z. Wang, X. Li, L. Wang and H. Wang, *J. Mater. Chem. A*, 2021, **9**, 16411–16417.

4 G.-F. Chen, Y. Yuan, H. Jiang, S.-Y. Ren, L.-X. Ding, L. Ma, T. Wu, J. Lu and H. Wang, *Nat Energy*, 2020, **5**, 605–613.

5 Y. Xu, K. Ren, T. Ren, M. Wang, M. Liu, Z. Wang, X. Li, L. Wang and H. Wang, *Chem. Commun.*, 2021, **57**, 7525–7528.

6 G. Ma, F. Sun, L. Qiao, Q. Shen, L. Wang, Q. Tang and Z. Tang, *Nano Res.*, 2023, **16**, 10867–10872.

7 Q. Gao, B. Yao, H. S. Pillai, W. Zang, X. Han, Y. Liu, S.-W. Yu, Z. Yan, B. Min, S. Zhang, H. Zhou, L. Ma, H. Xin, Q. He and H. Zhu, *Nat. Synth*, 2023, **2**, 624–634.

8 X. Zhou, W. Xu, Y. Liang, H. Jiang, Z. Li, S. Wu, Z. Gao, Z. Cui and S. Zhu, *ACS Catal.*, 2024, **14**, 12251–12259.

9 F. Dou, F. Guo, B. Li, K. Zhang, N. Graham and W. Yu, *Journal of Hazardous Materials*, 2024, **472**, 134522.

10 J. Zhao, L. Liu, Y. Yang, D. Liu, X. Peng, S. Liang and L. Jiang, *ACS Sustainable Chem. Eng.*, 2023, **11**, 2468–2475.